Chapter 3
Experimental

3.1 The UHV Chamber and the LT-STM

The Ultra High Vacuum (UHV) chamber and the LT-STM used in this work have been built by K. Schaeffer, S. Zöphel, and G. Meyer.[75-78] The UHV chamber is shown in Fig. 3.1. It consists of two parts separated by a valve: The preparation chamber and the measuring chamber, containing the LT-STM.

The preparation chamber is equipped with an ionisation gauge and a quadrupol mass spectrometer for rest gas analysis, an ion gun and a gas inlet system (Ne) for sputtering the sample, a Low Energy Electron Diffraction (LEED) system for characterization of the sample, and an evaporator (Kentax TCE-BS) for molecular beam epitaxy (MBE) of organic molecules. The evaporator consists of four quartz glass crucibles each one heated by a surrounding tungsten wire and equipped with Ni/Cr-Ni-thermocouples. A shutter closes all cells beside the one that is in use. The evaporator can be retracted and transferred to air for changing the substances and transferred back to the chamber, without breaking the vacuum in the UHV chamber. A load lock is attached to the preparation chamber for changing samples and a storage system inside the preparation chamber can store up to two samples. The turbo-molecular pump of the load lock is also used for pumping the UHV chamber during sputtering or bake out. Otherwise the UHV chamber is pumped

by an ion getter pump and a titanium sublimation pump (TSP); the base pressure is about 1×10^{-10} mbar.

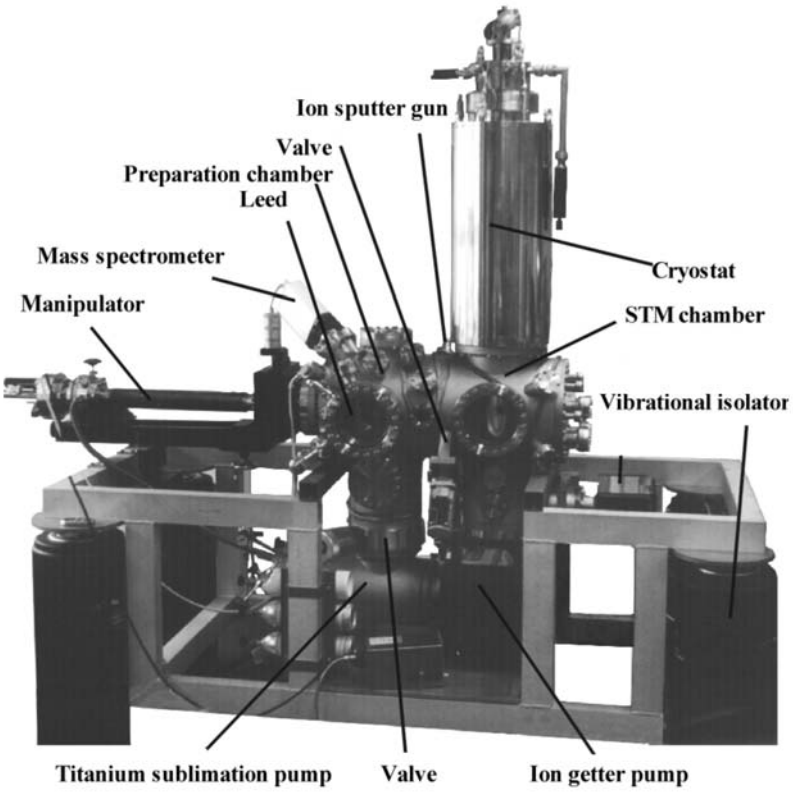

Fig. 3.1. The UHV chamber. The preparation chamber is to the left and the STM-chamber is to the right.[78] The MBE cell and the load lock are on the opposite side at the preparation chamber.

The samples are mounted on sample holders, attached to a button heater and a Ni/Cr-Ni-thermocouple (see Fig. 3.2). The sample holder can be transferred to the interlock, the sample storage, and the STM by means of a manipulator. The manipulator allows movement in all directions and rotation around its length axis and is also used to bring the sample into the different positions needed for preparation and characterization. Besides heating by means of the button heater, the sample can be cooled on the manipulator to approximately 15 K using liquid helium.

The measuring chamber contains another ionization gauge and the LT-STM. The LT-STM is cooled by a bath cryostat consisting of a liquid nitrogen tank (13.3 litre) and a liquid helium tank (4.3 litre). In the usual working mode the sample is maintained at a temperature of (8±1) K and the nitrogen and helium tanks have to be refilled every 44 hours. The STM is thermal weakly coupled to the cryostat and can be heated up to room temperature using a Zener-diode. For mechanical isolation the STM is hanging on stainless steel springs and is damped by an eddy current break. For further damping, especially against low frequency vibrations, the whole chamber sits on four pneumatically damped feet.

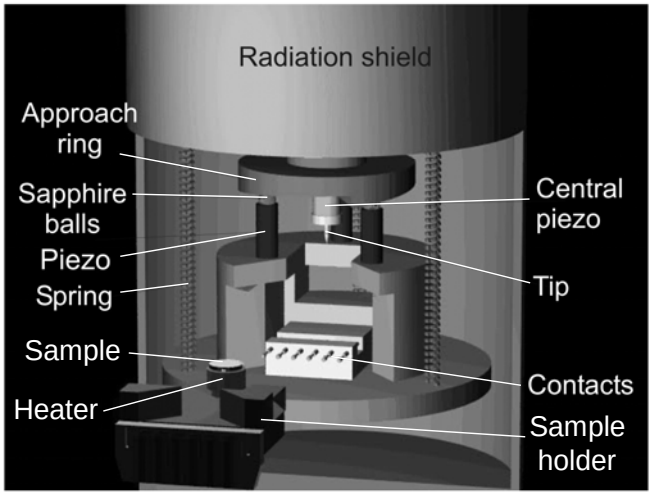

Fig. 3.2. Drawing of the STM inside the radiation shields.[78] The piezoelectric tubes and contact pads indicated. The sample holder can be seen in the front.

The STM is a modified Besocke type[79, 80] (Fig. 3.2). Three outer tube piezos and one central tube piezo are used to move the tip. The tip sits at the end of the central piezo, which is mounted on a plate with three ramps. The ramps rest on sapphire balls on the three outer piezos. By employing the three outer piezos und using slip-stick-motion, the tip is moved on the mm scale as needed for the coarse approach. When the tip is in tunnelling contact with the sample, the central piezo is employed to regulate the tip height (*z*-direction). The scanning movement

parallel to the sample (*x*- and *y*-direction) can be done either by the central piezo (*main* scanning mode) or by the outer piezos (*coarse* scanning mode). The latter mode was usually used in this work. The tunnelling current is measured at the tip side while the bias voltage is applied to the sample, i.e. the bias always refers to the sample with respect to the tip.

The STM is controlled by a PC using a homemade software program (PSTMAFM). The computer is connected to the analog electronics by a DSP (digital-signal-processor) and a D/A-A/D converter (digital-to-analog and analog-to-digital). The electronics consists of a high voltage amplifier for the movement of the piezos, a buffer amplifier for the tunnelling bias voltage, an amplifier for the tunnelling current and a lock-in amplifier, used for STS (scanning tunnelling spectroscopy). The D/A converters are used to control the piezos and the tunnelling voltage, while the A/D converters are used to read out the amplified tunnelling current and the lock-in signal.

All STM images shown in this work have been measured at temperatures between 7.3 K and 9 K and the piezo constants have been calibrated temperature dependent using the lattice parameters of the Cu(111) and the Cu(211) surface in atomically resolved images. For a more detailed description of the LT-STM see Ref. [78].

3.2 The Substrates

3.2.1 Cu(111)

The Cu(111) surface is the hexagonal close packed face of a Cu single crystal, which has a face centred cubic (fcc) structure with a lattice constant of $a = 3.61\text{Å}$.[81] The work function of Cu(111) is 4.94 eV.[82] The nearest neighbour distance is $a/\sqrt{2} = 2.55\text{Å}$ and the single step height is $a/\sqrt{3} = 2.08\text{Å}$. Later in this work step dislocations will be produced, therefore it is important to know that gliding preferentially occurs along the <110> slip systems leading to dislocation steps of height $n \times 2.08\text{Å}$ on the surface. There are two unequal types of such steps, i.e. A-type steps, exhibiting {100} facets and B-type steps, showing {111} facets, respectively. Once the exact orientation of the crystal is known, these steps can be distinguished by their orientation. The orientation of the crystal can be determined by means of STM, by observing the orientation of steps of 1/3 and 2/3 of the usual step height.[83] In Fig. 3.3 an atomically resolved STM image of the Cu(111) surface is shown, as used for calibration of the piezos in this work.

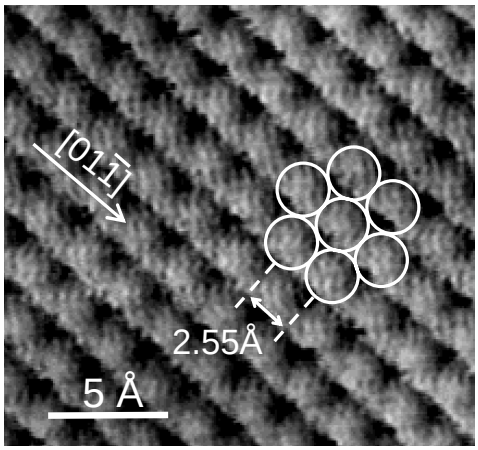

Fig. 3.3. STM image of the Cu(111) surface with atomic resolution. Tunnelling parameters are $I = 4.4\times10^{-7}$ A, U = -50 mV, T = 7.5 K. A hexagonal unit cell is indicated.

As all noble metal (111) surfaces, Cu(111) exhibits a Shockley surface state.[84] Surface states exist on the close-packed faces of noble metals, because of a band gap along the *Γ-L* direction of their bulk band structure.[84, 85] Due to the presence of the crystal surface, bulk forbidden electronic single-particle states arise, leading to a band in the corresponding projected bulk band gap. Thus a 2D nearly-free electron gas is formed by the Shockley state, which can be directly imaged as standing wave patterns by STM, as first observed by Eigler et al.[86, 87] (see Fig. 2.3). The otherwise half filled surface state is populated/depopulated by electrons tunnelling from/to the tunnelling tip. These electrons are scattered at defects as adsorbates or step edges causing interference patterns. Heller et al. proposed a multiple scattering method to simulate the observed standing wave patterns[88], which will be also applied in this work (see section 5.3). The dispersion relation of these surface state electrons could be determined with high accuracy by STS measurements and was found to be almost free electron like.[89] The band edge energy is E_Γ = -420 eV (with respect to the Fermi level) and the effective mass is $m^* = 0.40\ m_e$. Significant deviations from parabolic dispersion appear at energies higher than 2 eV above the Fermi level.[89] Moreover, lifetime[90] of surface state electrons, as well as scattering phase shifts and absorption coefficients for various systems have be determined.

3.2.2 Cu(211)

A model of the Cu(211) surface is shown in Fig. 3.4. The surface ideally consists of (111) facets separated by (100) steps running into the $[01\bar{1}]$ direction. The intrinsic steps, showing a distance of a_2 = 6.26 Å, are usually resolved in STM measurements, while atomic resolution along the close-packed step edges (a_1 = 2.55 Å), as in Fig. 3.5 is only obtained by a modified tip.

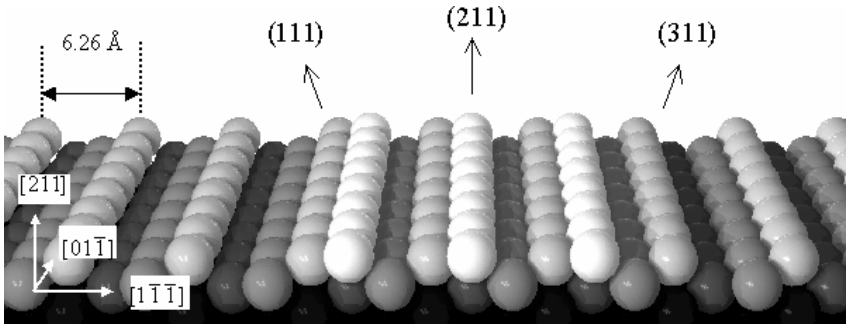

Fig. 3.4. Sphere model of the Cu(211) surface with a (111) and a (311) terrace step. The crystalline faces of the micro facets are indicated.

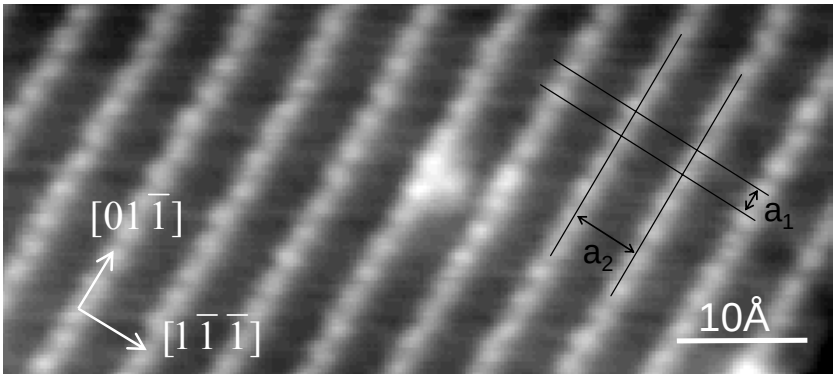

Fig. 3.5. STM image of the Cu(211) surface with atomic resolution. Tunnelling parameters are I = 3.8 nA, V = 86 mV, T = 7.3 K. In the centre of the image a single adatom is visible. The surface lattice parameters a_1 = 2.55 Å and a_2 = 6.26 Å are indicated.

The step separation is 6.26 Å and the miscut angle towards the (111) plane is 19.5°. Terrace step edges run preferably in $[01\bar{1}]$ direction, that is parallel to the intrinsic steps. The height of a single step is 0.74 Å. It can be distinguished between two different types of $[01\bar{1}]$ directed terrace steps. As illustrated in the model in Fig. 3.4, the (111) steps lead upwards while the (311) steps lead downwards with respect to the $[1\bar{1}\bar{1}]$ direction.

3.3 The Molecules

The molecules that are investigated in this work have all been synthesised by A. Gourdon and collaborators at the Nanoscience Group, CEMES-CNRS, Toulouse, France. The molecules are specially designed to study the possibilities of employing single molecules as electronic devices or as nano-machines. From the initial stage on, there have been intense collaborations between chemists and theoreticians in Toulouse and experimentalists in our group to develop these molecules.

3.3.1 Lander Type Molecules

Lander type molecules were specially designed to study single molecular wires on metallic surfaces by STM.[91] The Lander, also called Single Lander (SL, $C_{90}H_{98}$) consists of a planar polyaromatic molecular board, that constitutes the wire part, and four spacer groups, which are attached to the wire in order to decouple it from the metallic surface underneath (the molecule has been named due to similarities with landing interplanetary space crafts).

The molecular board is a polyaromatic planar system with overlapping π-orbitals. A HOMO-LUMO gap of $E_g = 1.24$ eV has been calculated for an Oligo(cyclopenta-naphto-flouroathene) molecular wire, as the Lander molecular board, by Magoga and Joachim.[92] At low bias voltage (inside E_g) they predicted the conductance G of a metal-molecule-metal junction to follow an exponential law

$$G = G_0 \exp(-\gamma L), \tag{3-1}$$

where L is the inter-electrode separation, γ is the inverse damping length, depending only on the intrinsic electronic properties of the molecular wire, and the prefactor G_0 is depending on the adsorption geometry of the molecule at the metal electrodes. In the case of an Oligo(cyclopenta-naphto-flouroathene) molecular wire, the two important parameters have been calculated by means of ESQC to be $\gamma = 0.207$ Å^{-1} and $G_0 = 1.27 \times 10^{-7}$ Ω^{-1}. [92] Although these values show

a rather large resistance of the molecular wire, the use of oligomers of well defined length is still promising because it permits the synthesis of nano-devices by including the chemical functionality in the wire.[92]

The four spacer groups (legs), attached to the board by insulating σ-bonds, are 3,5-di-*tert*-butyl-phenyl (TBP) groups. Fig. 3.6 shows the Lander molecule, which is approximately 17 Å long (in the direction of the molecular board) and 15 Å wide including van-der-Waals radii. The design ensures the board to be elevated from a flat surface, therefore reducing the interaction of the wire part with the surface and allowing lateral manipulation with the STM tip. Moreover, the molecule has a rigid aromatic platform (naphthalene end group) located beyond the spacers, which can be employed to study the electric contact of the wire with a nanostructure or step edge on a metal surface.

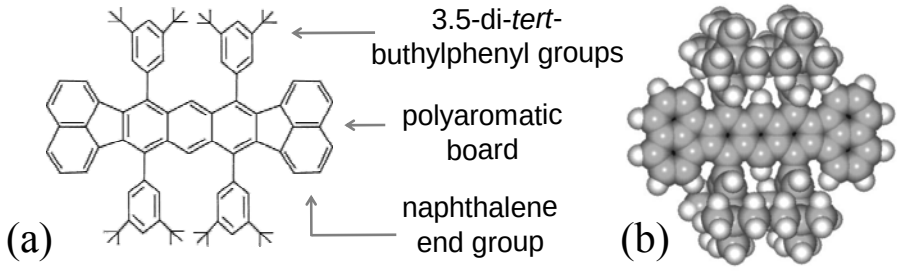

Fig. 3.6. Chemical structure of a Single Lander (a), with the important functionalized parts indicated. Sphere model (b) of the molecule in the gas phase conformation.

First STM experiments with Lander molecules have been performed on Cu(100) at room temperature in the group of Gimzewski at IBM Zürich.[16] Recently, the adsorption of Lander molecules on Cu(100) has been described in detail by Kuntze et al.[93] Many observations are characteristic for Lander molecules in general and remain valid for other Cu substrates: Cu(110)[94-96], Cu(111)[97] and Cu(211)[98]. These general results are reviewed in the following.

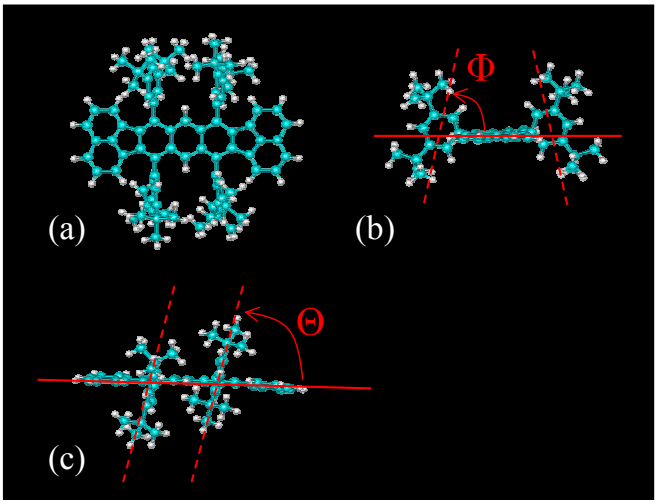

Fig. 3.7. Sphere models of a Lander molecule: (a) top view, (b) front view, (c) side view. The angles describing the deformation of the σ-bonds are indicated. Rotation out of the molecular plane is labelled Θ, bending of the σ-bonds is described by Φ.

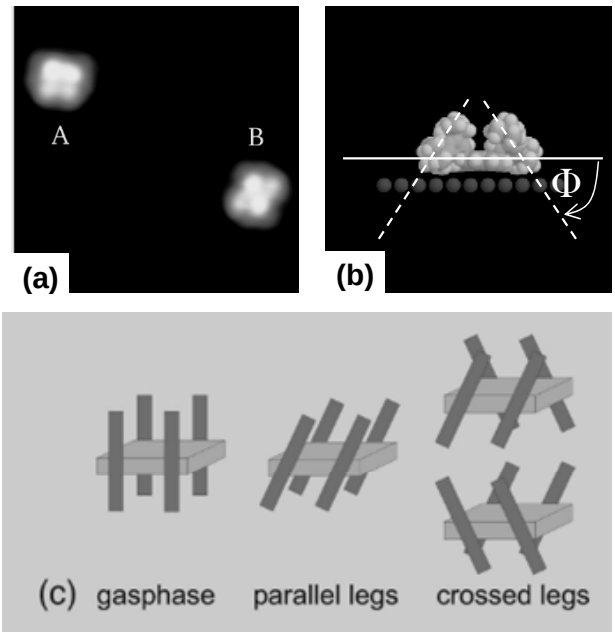

Fig. 3.8. Lander molecules adsorbed on a Cu(100) terrace. (a) STM image, I = 0.1 nA, U = 1.0 V, T = 4.6 K. Image size (9 nm)². Molecules in (A) parallel legs and (B) crossed legs conformation. (b) Ball model, the molecule is viewed from the front. (c) Illustration of the schematic conformations. The molecule is symbolized as a board with four legs (TBP-groups) attached. From ref.[93]

Lander molecules are imaged as four bright lobes corresponding to the four TBP side groups of the molecule, while the molecular board contributes little to the tunnelling current. Therefore the molecular board is normally not visible in STM images, as shown in Fig. 3.8(a).

On defect free terraces, Lander molecules are found in two different conformations, called crossed legs and parallel legs. Due to the molecule-substrate interaction, the conformation of the molecule is altered with respect to its gas phase conformation. The board to surface distance decreases from 5 Å, which would be expected for the gas phase conformation, to 3.7 Å for the adsorbed molecule. The main deformation is due to tilting and bending of the σ-bonds between molecular legs and board. The bending of the σ-bonds, allowing a decreased board-substrate distance, can be seen in the model in Fig. 3.8(b). The rotation of the legs can occur in different directions for the pairs of legs on each side of the board, as is indicated in models in Fig. 3.8(c), giving rise to the different conformations. The two legs on one side of the board are always rotated in the same direction owing to steric hindrance. The parallel legs conformation corresponds to a rotation of the legs on both sides of the board in the same direction and the molecule is imaged in an overall square shape. If the legs on both sides of the board rotate in opposite directions the molecule is adsorbed in the so called crossed legs conformation and is imaged in an rhombic shape. A third conformation is a mirror symmetric enantiomer of the latter. Although the molecule is not chiral in the gas phase, chirality is induced by adsorption and the anti-symmetrical rotation of legs.

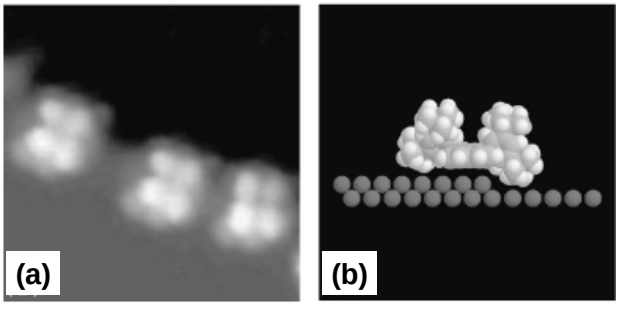

Fig. 3.9. Lander molecules adsorbed at a monoatomic step. (a) STM image: I = 0.1 nA, U = 1.0 V, T = 4.6 K. Image size (6.7 nm)². (b) Ball model, the molecule is viewed from the front. The molecular board is parallel to the step.[93]

The adsorption of Lander molecules at monoatomic step edges of the Cu(100) surface occurs with the molecular board parallel to the step, with two legs located on the lower and two legs on the upper terrace, as shown in Fig. 3.9.[93]

On Cu(110) a surface induced restructuring was observed by Besenbacher and collaborators[95, 96], consisting of double rows of Cu adatoms under the board of Lander molecules. The restructuring was proven by laterally manipulating Lander molecules away from their adsorption sites, as shown in Fig. 3.10. The nanostructure formed under the Lander molecule is (8±1) atoms long and two atoms wide.

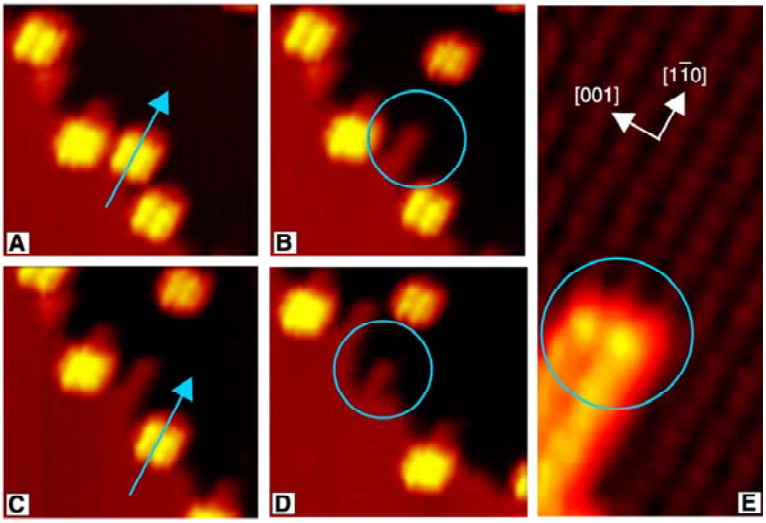

Fig. 3.10. (A to D) Manipulation sequence of the Lander molecules from a step edge on Cu(110). The arrows show which molecule is being pushed aside; the circles mark the tooth-like structures that are visible on the step where the molecule was docked. Scan parameters: I = 0.47 nA, U = 1.77 V, T = 100 K. Image size (13 nm)². Manipulation parameters: I = 1.05 nA, U = 55 mV. (E) STM image showing the characteristic two-row width of the tooth-like structure after removal of a single Lander molecule from the step edge (I = 0.75 nA, U = 1.77 V, image size 2.5 × 5.5 nm²). From ref.[96]

Besides the described SL (Fig. 3.11(a)) other Lander derivatives have been synthesized. Two of them have been investigated in the present work; they are called Reactive Lander (RL, $C_{94}H_{98}$, Fig. 3.11(b)) and Violet Lander (VL, $C_{108}H_{104}$, Fig. 3.11(c)). After synthesis the molecules are in the form of a orange, red, and violet crystalline powder in case of the SL, RL, and VL, respectively (therefore the naming of the VL). All these Lander type molecules exhibit four

identical lateral di-*tert*-butyl-phenyl "leg" groups (TBP) which hold the wire parallel to the metal surface. The molecular wire "board" is an aromatic planar conjugated π-system in all cases, but has different lengths for the different Lander type molecules: 17 Å for the SL, 20 Å for the RL, and 25 Å for the VL, respectively. The width of all molecules is approximately 15 Å.

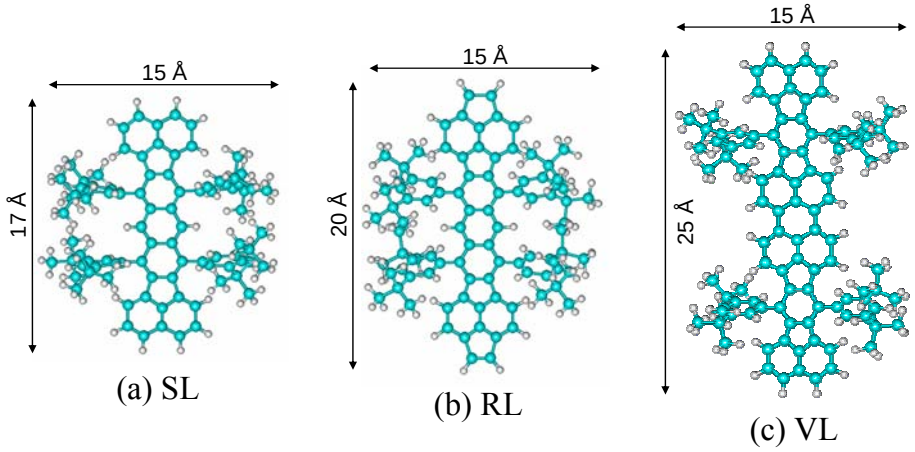

Fig. 3.11. Structure models and van der Waals dimensions of the different types of Lander molecules. Single Lander (SL), Reactive Lander (RL), and Violet Lander (VL). The aromatic board of the RL is extended at the ends with respect to the SL, while the board of the VL is extended in the middle part. The four di-*tert*-butyl-phenyl side groups (legs) are identical for all three molecules.

The idea behind the synthesis of the RL molecule was to add reactive sites to the ends of the molecular board in order to connect single molecules to an extended molecular wire by means of STM induced chemical reactions. The coupling reaction would be a 2+2 cyclo-addition. However, we found that the geometric conformation which is required for the reaction (the end groups above each other) could not be obtained when the molecules are adsorbed.

In case of the VL molecule[99], the wire part of a molecule is extended and the spacing between the legs is increased, reducing the steric hindrance between the molecular legs. Adsorption of the VL molecule was studied on Cu(100)[99], Cu(110)[100], and Cu(111)[101]. In the case of VL/Cu(110) it has been demonstrated by Otero et al. that the diffusion of VL molecules can be switched on and off by STM induced molecular orientations.[102]

3.3.2 HBC, HPB, and Derivatives

In the second part of this work, self-ordered processes of organic molecules are investigated. This is a technological important issue, since self-assembled organic thin films have numerous applications, e.g. in heterogeneous catalysis[103], sensors[104], and as interfaces in medical implants[105]. In terms of the economic fabrication of nano-structured surfaces and ordered thin films needed in molecular electronic and optic devices[104], self-assembly appears to be a practical strategy since it allows fabrication in a parallel geometry. Hence, for the design of molecules for applications in organic film technology, knowledge on the correlation between the chemical molecular structure and the monolayer epitaxial growth is of high interest.

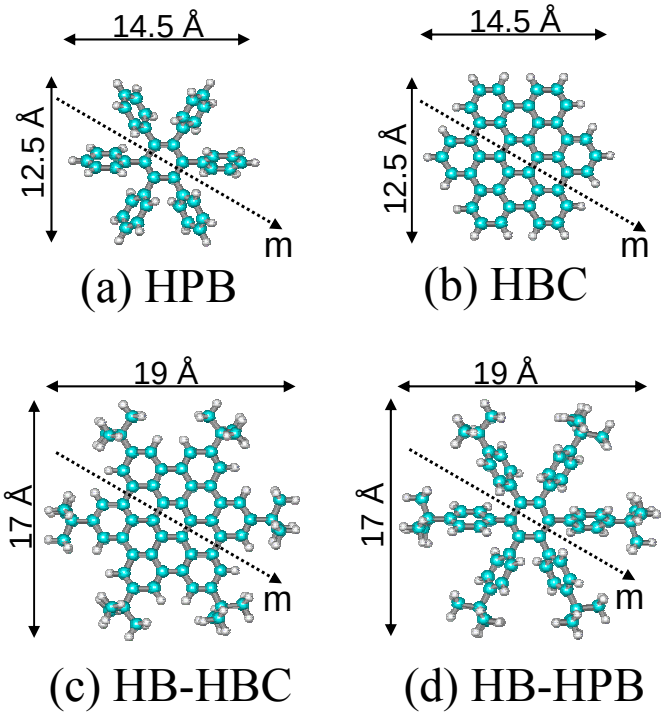

Fig. 3.12. Structure models and van der Waals dimensions of the investigated molecules. The dashed arrows indicate the molecular axis $\vec{m}$. (a) HPB, due to steric interaction the outer phenyl rings are tilted around the sigma bonds to the central benzene ring; (b) HBC, an entirely planar aromatic system; (c) HB-HBC and (d) HB-HPB are both equipped with six additional *tert*-butyl groups at the outer aromatic rings and have the same internal structure as (b) and (a) respectively.

The aim here is to study the effect of specific chemical groups on adsorption, growth, and self-ordering of large organic molecules. In this work four slightly different molecular derivates are chosen. This molecules are hexa-*peri*-hexabenzocoronene derivatives, which have been proved interesting for organic film photovoltaic technology[106] and molecular electronics[107-111].

The molecules are all showing a six-fold symmetry, therefore matching the Cu(111) substrate symmetry. Also the distances within the molecule, i.e. (2.5±0.1) Å between adjacent benzene rings, fit the lattice constant of Cu(111): 2.55 Å. The molecules, which are investigated here are: Hexa-*peri*-hexabenzocoronene (HBC, $C_{42}H_{18}$), hexa-*tert*-butyl-hexabenzocoronene (HB-HBC, $C_{66}H_{66}$), hexaphenylbenzene (HPB, $C_{42}H_{30}$), and hexa-*tert*-butyl-hexaphenylbenzene (HB-HPB, $C_{66}H_{78}$). The corresponding structure models are shown in Fig. 3.12.

The HBC molecule is well known in literature[32, 112-115], while the other molecules have been specially synthesised for this work by A. Gourdon. Highly ordered layer by layer growth of HBC has been shown upon deposition onto pyrolytic graphite (0001) and on molybdenum disulfide, MoS_2(0001).[116] This growth mode continues up to a layer thickness of at least 10 nm.[114] HBC has been studied in monolayer and multilayer coverage also on various noble metal surfaces, e.g. Au(111)[32, 113, 115], Au(100)[117], and Cu(111)[32]. Generally, on clean metals (under UHV conditions) the formation of highly ordered monolayers with the HBC molecular planes oriented parallel to the substrate has been reported. Higher coverage leads to columnar stacking of HBC molecules with highly oriented HBC-adlayers up to a thickness of 2 nm on Cu(111) and Au(111).[32]

The Hexa-*peri*-hexabenzocoronene (HBC) is a large molecular segment of a graphite plane, which can be deposited using sublimation. The molecule is large enough to add functional molecular side groups, making these class of molecules very interesting for applications. Self-organization of hexaalkyl-substituted derivates of HBC into a columnar mesophase in organic solvents has been demonstrated, leading to one-dimensional conductors with a very high charge carrier mobility, i.e. molecular nanowires[108]. Recently, Jäckel et al. reported on a

prototypical single-molecule chemical-field-effect transistor, using an HBC derivative in the tunnel junction of an STM.[111] Moreover, discrete tubular self-assembled nano-tubes have been grown from HBC derivatives.[109]

The hexaphenylbenzene (HPB) molecule is a pre-stage in the synthesis of the HBC molecule. In case of the HPB, the bonds between the outer phenyl rings are not established in comparison to HBC. Hydrogen atoms are bond to the corresponding carbon atoms inducing steric hindrance between adjacent phenyl rings. In vacuum, all phenyl groups are rotated around their σ-bonds by approximately 45° with respect to the central benzene ring, leading to a propeller shape form of the molecule. It has been shown that HPB can be transferred into HBC by thermic cyclodehydrogenation on a Cu(111) surface.[118]

In case of the larger HB-HBC and HB-HPB molecules, *tert*-butyl side groups are added to the previously described HBC and HPB molecules. These side groups are similar to the di-*tert*-butyl side groups, that are used in the case of the Lander molecules. The adding of such side groups is expected to alter the intermolecular forces of adsorbed molecules and therefore to influence molecular ordering. Large differences in the adsorption and monolayer structure have been observed due to the adding of *tert*-butyl side groups in the case of decacyclene (DC) and hexa-*tert*-butyl decacyclene (HB-DC) on Cu(110) as has been shown by Schunack and collaborators.[27, 28]

3.4 Sample Preparation

The sample substrates are prepared by multiple cycles of sputtering with 1.3 keV Ne ions at room temperature for 20 minutes followed by annealing to 770 K for five minutes. The molecules are evaporated from a home built Knudsen cell and from commercial Knudsen cells (Kentax TCE-BS). The evaporation temperatures of the molecules are shown in Table 3.1.

Molecule	Chemical formula	Sublimation temperature (±20 K)
SL	$C_{90}H_{98}$	620 K
RL	$C_{94}H_{98}$	650 K
VL	$C_{108}H_{104}$	660 K
HBC	$C_{42}H_{18}$	620 K
HB-HBC	$C_{66}H_{66}$	570 K
HPB	$C_{42}H_{30}$	420 K
HB-HPB	$C_{66}H_{78}$	520 K

Table 3.1. Chemical formulas and used sublimation temperatures for the investigated molecules. The sublimation temperatures correspond to an evaporation rate of 10^{-4} ML/s.

The preparation is monitored via a quartz crystal microbalance, that has been calibrated using the STM. The sensibility of the microbalance is in the order of 5×10^{-4} monolayer (ML) and the error in the coverage is about 30% as checked by STM. In this work 1 ML is defined as the amount of molecules, that would cover the sample completely assuming the densest observed monolayer structure. In all cases the preparations are in the submonolayer regime, a typically adsorbed dosage is 0.01 ML, the typical evaporation time is 10 min. For investigations of monolayer formation (i.e. in the case of HBC derivates) sometimes a higher coverage, up to 0.3 ML is chosen, while for the investigation of standing wave patterns and manipulation experiments with single molecules a lower coverage, in

the order of 1×10^{-3} ML is used. In these cases the evaporation time is kept at values between 5 and 15 minutes, but the evaporation temperature is varied, using the calibrated microbalance to achieve the desired flux (i.e. evaporation rates are in the orders of 10^{-6} ML/s to 10^{-3} ML/s). At the sublimation temperature the flux increases by about one order of magnitude with a temperature increase of 10 K. It is important to mention that the size of the molecules that can be evaporated by molecular beam deposition from a hot crucible is limited. In general, the sublimation temperature of molecules, which are only loosely bound by van der Waals forces, increases with the molecular weight. As shown in Table 3.1 the HBC molecule is an exception to this general rule since HBC molecules grow in layers like graphite thus increasing the sublimation temperature due to the rather strong van der Waals forces between the molecular planes. If the temperature needed for sublimation of the molecule is higher than the temperature at which the inner molecular bonds dissociate, molecules are evaporated in fragments. This critical temperature seems to be nearly reached in the case of the Violet Lander (VL), the largest molecule investigated in this work. A crucible temperature of at least 660 K was needed to evaporate the VL molecules and STM measurements show that a large amount of fragments were sublimed together with intact molecules.

Another important preparation parameter is the sample temperature. When the sample temperature is low enough, molecular diffusions is frozen in and molecules are pinned at their initial adsorption places. For dosages in the far submonolayer regime, this will result in a random distribution of single molecules on the surface, useful for the investigation of single molecules and their properties as surface state scatterers. However, preparation at low sample temperature bears the disadvantage of increasing the sticking coefficient also for unwanted rest gas molecules, e.g. CO, which might contaminate the sample. On the other hand no contamination is observed inside the LT-SM within weeks, because of the cold shields surrounding the sample. Contamination is thus a problem only as long as the sample is inside the preparation chamber, especially when the sample temperature is low and the ambient pressure is increased due to the heating of the Knudsen cell. At higher sample temperatures, molecules can diffuse until they reach preferred adsorption sites. This can result in selective adsorption at certain

substrate sites, molecular self-organisation, or, involving also the diffusion of substrate atoms, molecular induced restructuring.

Since the manipulator allows cooling and heating the sample, the molecular adsorption could be investigated temperature dependent. Therefore, sample temperatures were chosen between 70 K, freezing in the diffusion of SL molecules, and 330 K, allowing surface diffusion of all investigated molecules. The ambient pressure during evaporation is in the order of 10^{-9} mbar. After preparation the sample is cooled down to 20 K on the manipulator and transferred to the STM. All shown STM images have been measured at temperatures between 7 K and 9 K.